PROGRESS IN COLOR, COLORANTS AND COATINGS

available online @ www.pccc.icrc.ac.ir

Prog. Color Colorants Coat. 10 (2017), 141-148

Ministry of Science, Research and Technology
Institute for Color Science and Technology

Synthesis and Characterization of Two Green Nanopigments Based on Chromium Oxide

A. Babaei Darani, M. Khajeh Aminian*, H. Zare
Department of Physics, Yazd University, P. O. Box: 89195-741, Yazd, Iran

ARTICLE INFO

Article history:
Received: 08 Jan 2016
Final Revised: 04 Apr 2017
Accepted: 09 Apr 2017
Available online: 13 Jun 2017

Keywords:
Polyol method
Green pigment
Cr_2O_3
$CoCr_2O_4$

ABSTRACT

*Green nano pigments of Cr_2O_3 and $CoCr_2O_4$ were successfully prepared by polyol method followed by calcination at 770 °C. The Cr_2O_3 and $CoCr_2O_4$ samples were characterized by X-ray diffraction (XRD), scanning electron microscopy (SEM), diffuse reflectance spectroscopy (DRS), dynamic light scattering (DLS), UV–Vis spectroscopy and CIEL*a*b* colorimetry methods. Dynamic light scattering analysis confirmed the formation of nanoparticles in suspensions. XRD data of Cr_2O_3 and $CoCr_2O_4$ powders displayed the formation of crystallized rhombohedral and spinel structures, respectively. The calculated average crystallite size of Cr_2O_3 and $CoCr_2O_4$ is ~54 and 39 nm, respectively. The SEM results showed that the average size of Cr_2O_3 and $CoCr_2O_4$ nano pigments is about 70-80 nm, while $CoCr_2O_4$ nano pigments were more agglomerated than Cr_2O_3. The calorimetric and DRS data confirmed the formation of green pigments in both samples. Prog. Color Colorants Coat. 10 (2017), 141-148© Institute for Color Science and Technology.*

1. Introduction

Inorganic pigments have been extensively used in the production of paints, plastics, building materials, glazes, ceramics coatings and glasses since ancient times [1-5]. The physical and optical property of inorganic pigments depends on the size, shape, refractive index and the composition of the pigment particles [1, 3, 6]. During the preceding decades, there is a growing interest in nano-sized pigments due to their high surface area which assures higher surface coverage and an increased number of reflectance points resulting in maximum scattering [7]. Smaller pigment particles can also enhance the stability of the suspension and the mechanical strength of the paint [1, 7-9].

Pigments based on chromium oxide, such as Cr_2O_3, $CoCr_2O_4$ and Al_2O_3-Cr_2O_3, have been of high interest due to the excellent performance in green color, high melting point, high oxidation, and excellent resistance to light [2, 10, 11]. Recently, they have been used in widespread applications such as ceramics, coatings, advanced colorants, plastic, refractories, printing and construction materials [1, 4, 5, 10-14]. By using chromium oxide based ceramic green nano-pigments, newer or improved applications have been possible [1, 5].

In recent years, various routes for preparation of chromium oxide nano pigments have been developed such as laser induced deposition, sol-gel technique [14,16], gas condensation [17], sonochemical reaction [18], microwave plasma [19], hydrothermal [3, 10], thermal decomposition [2, 4, 5], urea method [6], nano-casting method [17] and combustion synthesis [3, 22, 23]. Most of these routes involve one or more disadvantages, including complication, the use of expensive equipments, severe preparation conditions,

*Corresponding author: kh.aminian@yazd.ac.ir

and inhomogeneity (shape and size distribution) of the resultant particles.

A method shown to be quite effective for preparation of a suspension containing nano-sized oxide particles is so-called polyol method [3]. Polyol method is method of manufacture at low temperatures and during the reaction, aggregation is likely less. The final product is a stable suspension with particles smaller than 200 nm which can be used in ceramic printing industry. In this method, a high boiling point liquid such as ethylene glycol (EG), diethylene glycol (DEG), triethylene glycol (TREG) and tetraethylene glycol (TEG) is used as a solvent [3, 24]. Some additives are used as protecting or stabilizing agent [26], particle growth reducing agent for metallic ions [12, 25]. Synthesis of suspended crystalline nanoparticles in a solution is possible by polyol method, as high temperatures could be achieved during the reaction. Another advantage of this route is the possibility to kinetically control the reaction conditions [26].

The current paper aims to the synthesis of Cr_2O_3 and $CoCr_2O_4$ as green nano pigments using polyol method. The pigments were prepared as suspension and powder. The optical and structural properties of samples were also investigated.

2. Experimental

2.1. Synthesis of Cr_2O_3 and $CoCr_2O_4$ nanoparticles

Cobalt acetate tetrahydrate ($Co(CH_3COO)_2.4H_2O$, purity; 99%, Sumchon), chromium nitrate nonahydrate ($Cr(NO_3)_3.9H_2O$, purity; 98%, Sumchon), ethanol (purity; 96% , Merck) and DEG (purity; 99% , Merck) were used as precursor.

For preparation of Cr_2O_3 nano pigment, 0.299 g of $Cr(NO_3)_3.9H_2O$ (0.774 mmol) was dissolved in 30 mL of DEG and stirred for 10 min. The solution was refluxed at 140 ˚C for 1 h. Then 2 mL of distilled water was added to this solution and was refluxed at 180 ˚C for 12 h. The obtained dark green suspension was cooled down to room temperature. In order to separate pigment powder from the suspension, 30 mL ethanol was added to the resulting mixture. Then the powder was separated by centrifugation (10 min at 3800 rpm), dried at 100 ˚C, and then was heated at 770 ˚C for 4 h. The $CoCr_2O_4$ pigment was synthesized through the same route as above except that 0.806 g of $Cr(NO_3)_3.9H_2O$ and 0.248 g of $Co(CH_3COO)_2.4H_2O$ were used as the precursor.

2.2. Characterization of powders and suspensions

The optical properties of the suspensions and the powders were measured by employing UV-Vis spectrophotometer (Avantes Photodiode array spectrophotometry avaspec-2048 equipped with ava light-DH-S-BAL as the source). The particle size distribution and zeta potential of the suspensions were determined based on dynamic light scattering method using Zetasizer (Nano-ZS, Malvern Instruments). The size and morphology of the powders were determined using a scanning electron microscope (SEM, VEGA3 TESCAN). The X-ray diffraction (XRD) patterns of the powders were recorded using Philips X'Pert Pro machine (CuKα radiation: λ=1.5406 °A). In addition, L* a* b* color parameters of nano-pigments were measured following the CIE (Commission Internationale de l'Eclairage) colorimetric method using a portable spectrophotometer (X-Rite SP-64).

2.3. Application as ceramic inks

The ceramic printing process was carried out at Masoud Tile Company. Ceramics were glazed and suspensions were printed on ceramics by spray method. After printing, the samples were annealed at 1100 ˚C. The size and morphology of the printed nanopigments on ceramics were investigated using SEM.

3. Results and Discussion

The polyol method was used to prepare the Cr_2O_3 and $CoCr_2O_4$ nano pigments. Photographs of Cr_2O_3 and $CoCr_2O_4$ nano pigments synthesized by polyol rout and annealed at 770 ˚C are shown in Figures 1-a, 1-b. They are mostly in green. Figures 1-c, 1-d show SEM images of Cr_2O_3 and $CoCr_2O_4$ nanopigments annealed at 770 ˚C in the air atmosphere. Figure 1c shows that the Cr_2O_3 sample is composed of nanoparticles with the average size of ~ 70 nm which are agglomerated in a densely stacking style and made particles larger than 2 µm. Figure 1d shows SEM image of $CoCr_2O_4$ nanopigments indicating that nanoparticles are mostly spherical with an average size of 75 nm. There are also some agglomerated particles in the image. The size of the agglomerated particles for $CoCr_2O_4$ is less than that of Cr_2O_3. It seems that the agglomerated particles for $CoCr_2O_4$ have been formed during the drying process. It can be concluded from Figure 1 that Cr_2O_3 nanopigments are in the same size as $CoCr_2O_4$ nano

pigments, but are much more agglomerated.

SEM images of the bare ceramic and printed ceramics are shown in Figure 2. The morphology of glaze layer on ceramics is shown in Figure 2a. The surface is relatively smooth with small cracks. According to Figures 2b, 2c, the printed nanopigments on ceramics are homogeneous and nearly spherical with the particle sizes of 30-100 nm. Also, the average particle size of Cr_2O_3 and $CoCr_2O_4$ nanoparticles is 45 and 75 nm, respectively.

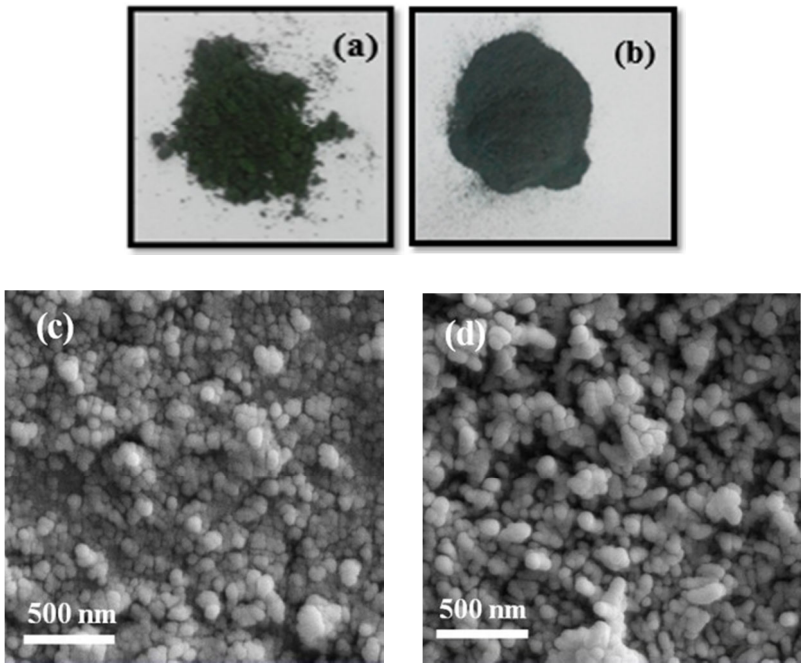

Figure 1: Photographs of (a) Cr_2O_3, (b) $CoCr_2O_4$ and SEM images of (c) Cr_2O_3, (d) $CoCr_2O_4$ nano pigments annealed in air at 770 ˚C.

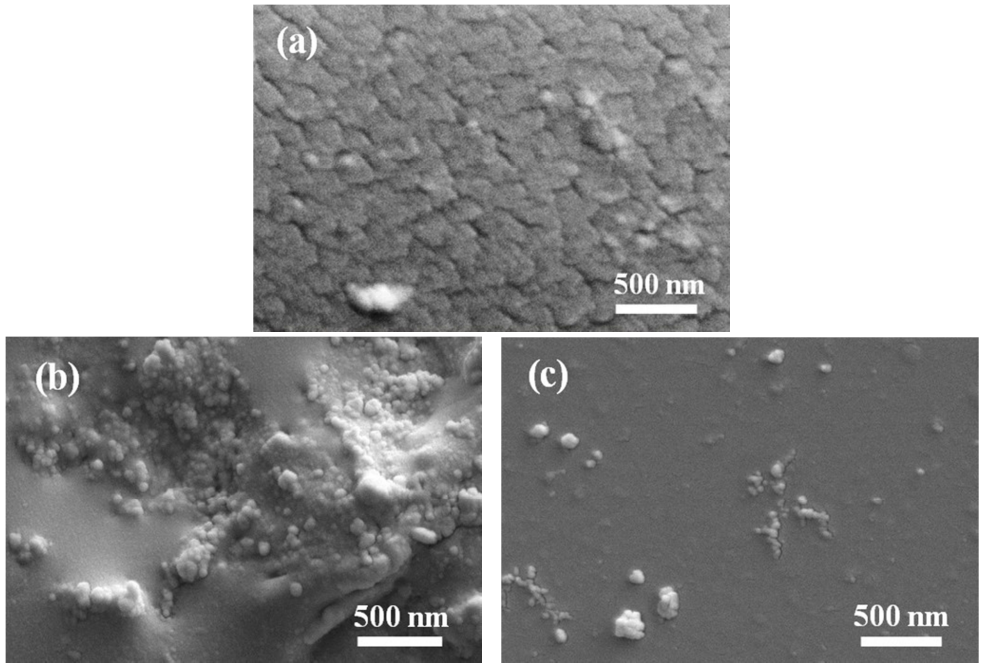

Figure 2: Scanning electron micrographs of bare ceramic (a), nano- Cr_2O_3 (b) and nano-$CoCr_2O_4$ printed ceramics (c), annealed at 1100 ˚C.

Figure 3 shows XRD patterns of Cr_2O_3 and $CoCr_2O_4$ nanopigments. Figure 3a is related to Cr_2O_3 nanopigments. It shows that all peaks can be indexed to the rhombohedral structure of Cr_2O_3 (JCPDS File No. 76-0147 with a= b= 4.9516 °A, c= 13.5987 °A, unit cell volume= 288.75 °A^3 and space group= R-3c) and no other phases such as CoO and Co_2O_3 can be observed. Eight important peaks are shown in this spectrum which are related to (012), (104), (110), (113), (024), (116), (214), (300) crystal planes. The crystallite size for all peaks was calculated by scherrer's formula. The average crystallite size is approximately 54 nm [14, 25].

XRD pattern of $CoCr_2O_4$ nanopigments is presented in Figure 3b. It shows that the pigments are single phase and the peaks correspond to the planes of spinel phase $CoCr_2O_4$ crystal (JCPDS-22-1084 with lattice size of 8.333 °A, unit cell volume = 578.63 °A and space group = Fd-3m) [15]. The average crystallite size calculated for the peaks corresponding to (111), (220), (311), (222), (400), (422), (511), (440) crystal planes was ~39 nm. The results show that the mean crystallite size of $CoCr_2O_4$ nano pigments is smaller than that of Cr_2O_3. A comparison of XRD and SEM data indicates that Cr_2O_3 and $CoCr_2O_4$ nanoparticles are consisted of crystallites with 54 and 39 nm, respectively.

The chemical reactions for the formation of Cr_2O_3 and $CoCr_2O_4$ nanoparticles are dependent on temperature and surrounding atmosphere. The mechanism of forming Cr_2O_3 nanoparticles is suggested as the following reactions [27].

$$Cr(NO_3)_3.9H_2O \rightarrow Cr(NO_3)_3.3H_2O + 6H_2O \quad (1)$$

$$Cr(NO_3)_3.3H_2O \rightarrow Cr(OH)_x(NO_3)_{3-x}.(3-x)H_2O + xHNO_3 \rightarrow Cr(OH)_3 + 3H_2O + 3HNO_3 \quad (2)$$

$$2\ Cr(OH)_3 \xrightarrow{\text{High temperature}} Cr_2O_3 + 3\ H_2O \quad (3)$$

The chemical reactions for the formation of $CoCr_2O_4$ nanoparticles can be considered as [28, 29]:

$$Co(CH_3COO)_2.4H_2O \rightarrow Co(CH_3COO)_2.2H_2O + 2H_2O \quad (4)$$

$$Co(CH_3COO)_2.2H_2O \rightarrow Co(OH)_x(CH_3COO)_{2-x}.(2-x)H_2O + xCH_3COOH \rightarrow Co(OH)_2 + 2CH_3COOH \quad (5)$$

$$Co(OH)_2 + 2Cr(OH)_3 \xrightarrow{\text{High temperature}} CoCr_2O_4 + 4H_2O \quad (6)$$

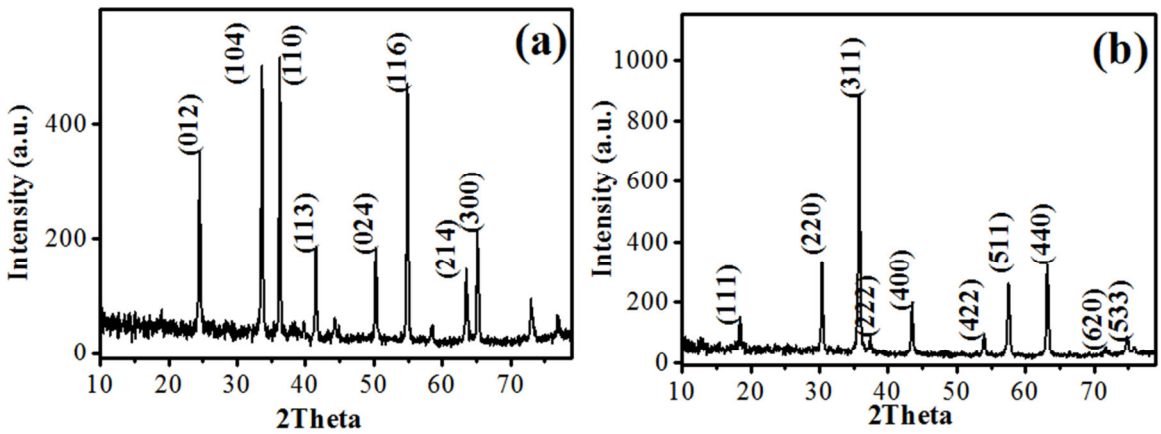

Figure 3: XRD patterns of (a) the Cr_2O_3, (b) $CoCr_2O_4$ nanopigments annealed at 770 ˚C.

The Color parameters (L*, a* and b*) of Cr_2O_3 and $CoCr_2O_4$ nanopigments are presented in Table 1. The yield of green color is mainly controlled by the parameter a*: a negative value for a* parameter indicates green color. On the other hand, L* component indicates the lightness of the pigment. The value of a* for Cr_2O_3 sample (~ -9.17) is less than that of $CoCr_2O_4$ sample (~ -8.17), therefore Cr_2O_3 sample shows higher intensity of green color, while the lightness (L*) of Cr_2O_3 sample is less than that of $CoCr_2O_4$ sample. The value of b* for Cr_2O_3 sample (~7.03) is more than that of $CoCr_2O_4$ sample (~0.34), which indicates that the intensity of yellow component of the color is less for $CoCr_2O_4$ sample.

Diffuse reflectance spectra of the powders are shown in Figure 4. The spectra show a broad band peak at 536 nm for Cr_2O_3 sample and at 527 nm for $CoCr_2O_4$ sample. It is well known that the peaks in the region of visible light belong to the green color.

The particle size distribution of Cr_2O_3 and $CoCr_2O_4$ suspensions was measured by dynamic light scattering (DLS) method and reported in Figure 5. According to Figures 5a and 5b, the particle size for Cr_2O_3 and $CoCr_2O_4$ samples varies in the range of 5-15 nm and 4-40 nm, respectively. The measured average particle size for Cr_2O_3 is about 9 nm, whereas it is about 16 nm for $CoCr_2O_4$. It seems that there are two different kinds of particles in the $CoCr_2O_4$ suspension; one in the range of 4-12 nm and the other in the range of 13-40 nm. It can be supposed that the bigger particles were formed by the agglomeration of smaller particles. Also, it can be observed that the average particle size for the suspension and the powder are different which may be due to the growth and agglomeration of particles after annealing at 770 °C.

According to this analysis, the mean particle size for S1 was found to be 9 nm and for S2 was 16 nm. Since the mean size for the suspended particles of both samples is smaller than the crystallite size of them, it can be concluded that some agglomeration and crystal growth have happened during the heating process (770 °C).

Table 1*:* Color parameters (L* a*b*) of the powders synthesized by polyol method and annealed at 770 ˚C.

Sample	Color Parameters		
	a*	b*	L*
Cr_2O_3	-9.17	7.03	35.70
$CoCr_2O_4$	-8.17	0.34	40.52

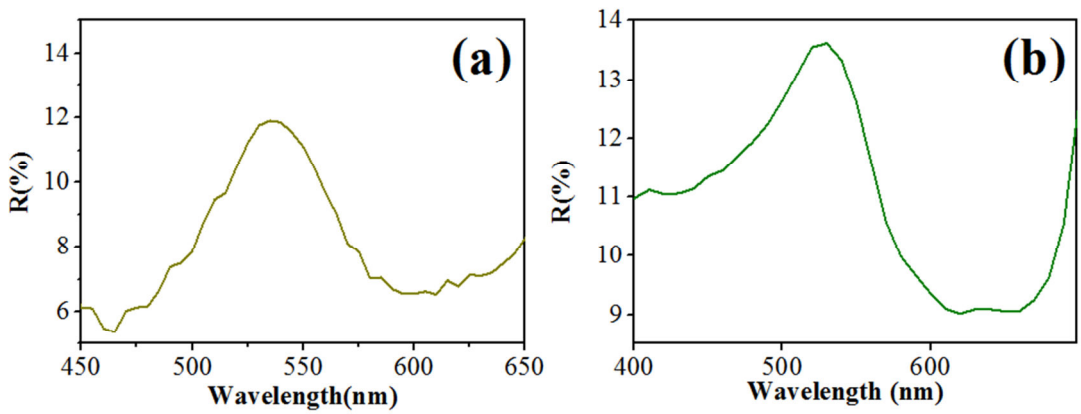

Figure 4: Diffuse reflectance spectra of (a) Cr_2O_3 and (b) $CoCr_2O_4$ green nano pigments.

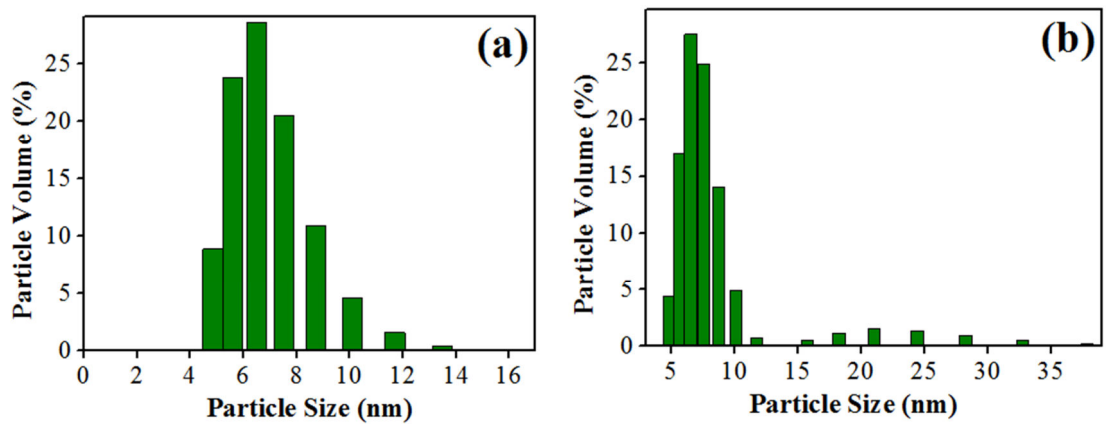

Figure 5: The particle size distribution of (a) Cr_2O_3 and (b) $CoCr_2O_4$ suspensions.

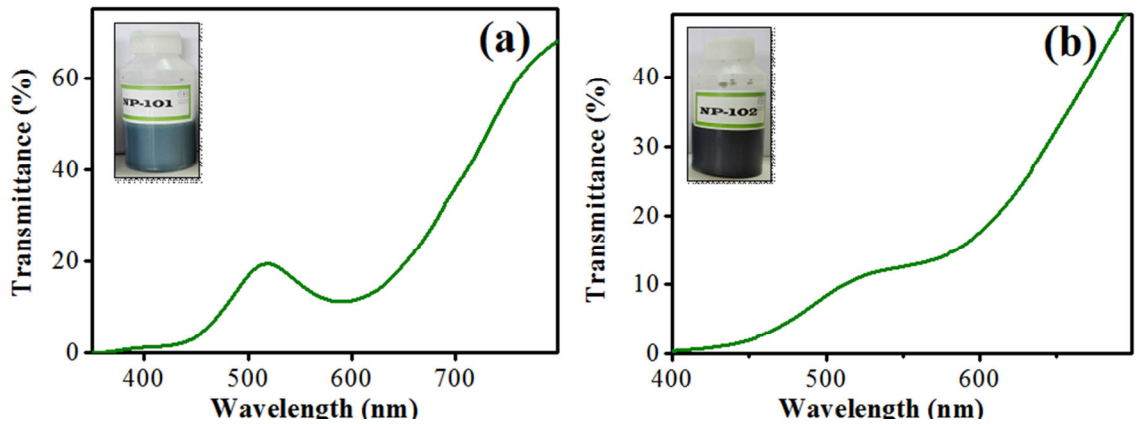

Figure 6: Transmission spectra of (a) the Cr_2O_3 (Inset: Photograph of the Cr_2O_3 suspension) and (b) $CoCr_2O_4$ suspension (Inset: Photograph of the $CoCr_2O_4$ suspension).

Figure 6 demonstrates the UV-Vis transmittance spectra of Cr_2O_3 and $CoCr_2O_4$ suspensions after refluxing. A single peak in green region is observed for both samples; at 517 nm and 532 nm for Cr_2O_3 and $CoCr_2O_4$, respectively. According to the results, the transmittance peaks in the green region of the spectra make the suspensions look green (see the insets in Figure 6).

The stability of suspensions and the density of the surface charge on the particles in a suspension are generally determined by measuring the zeta potential [30]. The measured zeta potential values for Cr_2O_3 and $CoCr_2O_4$ suspensions were about 6.31 and -23.6 mV, respectively. From the value 6.31 mV it can be found that due to the formation of double layer around the nanoparticles in suspension, the nanoparticles are positively charged in suspension. Given that the limit of the zeta potential for stable suspension is kT/e, this amount is less than the limit and agglomeration for the suspension is possible [30]. Therefore, the stability of the suspension may be insufficient. On the other hand, the value of -23.6 mV means that nanoparticles are negatively charged. The $CoCr_2O_4$ suspension has higher zeta potential value indicating that it is more stable than Cr_2O_3 suspension.

4. Conclusions

The present study reported the preparation and characterization of nanosized rhombohedral structure of Cr_2O_3 and spinel structure of $CoCr_2O_4$ green pigments. The synthesis of Cr_2O_3 and $CoCr_2O_4$ samples were successfully carried out by using polyol method. The results of DLS approved the formation of Cr_2O_3 and $CoCr_2O_4$ nanoparticles in the suspensions. According to XRD and SEM results, the crystalline nano pigments have been prepared and the

measurement of the color parameters reflected a green color for both samples. The average crystallite size of Cr_2O_3 and $CoCr_2O_4$ are calculated ~54 and 39 nm, respectively. The SEM results showed that the average size of Cr_2O_3 and $CoCr_2O_4$ nano pigments is about 70-80 nm. The results of the present study demonstrate that polyol route is an effective method to synthesize powder and liquid nano pigments. The $CoCr_2O_4$ suspension has higher zeta potential value indicating that it is more stable than Cr_2O_3 suspension.

Acknowledgement

The authors thank Masoud Tile Company of Iran for the instruments and technical assistance.

5. References

1. D. Rangappa, T. Naka, A. Kondo, M. Ishii, T. Kobayashi, T. Adschiri, Transparent $CoAl_2O_4$ hybrid nano pigment by organic ligand-assisted supercritical water, *J. Am. Chem. Soc*., 129(2007), 11061-11066.
2. S. T. Liang, H. L. Zhang, M. T. Luo, K. J. Luo, P. Li, H. B. Xu, Y. Zhang, Colour performance investigation of a Cr_2O_3 green pigment prepared via the thermal decomposition of CrOOH, *Ceram. Int.,* 40(2014), 4367-4373.
3. C. Feldmann, Preparation of nanoscale pigment particles, *Adv. Mater.,* 13(2001), 1301-1303.
4. H. L. Zhang, S. T. Liang, M. T. Luo, M. G. Ma, P. P. Fan, H. B. Xu, P. Li, Y. Zhang, Preparation and color performance control of Cr_2O_3 green pigment through thermal decomposition of chromium hydroxide precursor, *Mater. Lett.,* 117 (2014), 244-247.
5. S. Sangeetha, R. Basha, K. J. Sreeram, S. N. Sangilimuthu, B. U. Nair, Functional pigments from chromium (III) oxide nanoparticles, *Dyes Pigm.,* 94(2012), 548-552.
6. M. Ocana, Nanosized Cr_2O_3 hydrate spherical particles prepared by the urea method, *J. Eur. Ceram. Soc.,* 21(2001), 931-939.
7. S. Salem, S. H. Jazayeri, F. Bondioli, A. Allahverdi, M. Shirvani, A. M. Ferrari, $CoAl_2O_4$ nano pigment obtained by combustion synthesis, *Int. J. Appl. Ceram. Technol.,* 9(2012), 968-978.
8. J. H. Kim, B. R. Son, D. H. Yoon, K. T. Hwang, H. G. Noh, W. S. Cho, U. S. Kim, Characterization of blue $CoAl_2O_4$ nano-pigment synthesized by ultrasonic hydrothermal method, *Ceram. Int*., 38(2012), 5707-5712.
9. S. K. Biswas, D. Dhak, A. Pathak, P. Pramanik, Chemical synthesis of environment-friendly nanosized yellow titanate pigments, *Mater. Res. Bull.*, 43(2008), 665-675.
10. M. M. Abdullah, F. M. Rajab, S. M. Al-Abbas, Structural and optical characterization of Cr_2O_3 nanostructures: Evaluation of its dielectric properties, *AIP Advances*., 4(2014), 027121.
11. P. Li, H. B. Xu, S. L. Zheng, Y. Zhang, Z. H. Li, Y. L. Bai, A green process to prepare chromic oxide green pigment, *Environ. Sci. Technol.,* 42(2008), 7231-7235.
12. A. M. Ibrahim, M. A. El-Latif, M. M. Mahmoud, Synthesis and characterization of nano-sized cobalt ferrite prepared via polyol method using conventional and microwave heating techniques, *J. Alloys Compd*., 506(2010), 201-204.
13. W. Herbst, K. Hunger, Industrial organic pigments: production, properties, applications, John Wiley & Sons. (2006).
14. V. Balouria, A. Singh, A. K. Debnath, A. Mahajan, R. K. Bedi, D. K. Aswal, S. K. Gupta, R. Mittal, A. K. Chauhan, R. Mukhopadhyay, Synthesis and characterization of sol-gel derived Cr_2O_3 nanoparticles, InAIP Conference Proceedings-American Institute of Physics., 1447(2012), 341.
15. D. Gingasu, I. Mindru, D. C. Culita, L. Patron, J. M. Calderon-Moreno, P. Osiceanu, S. Preda, O. Oprea, V. Parvulescu, V. Teodorescu, J. P. S. Walsh, Structural, magnetic and catalytic properties of cobalt chromite obtained through precursor method, *Mater. Res. Bull.,* 62 (2015), 52–64.
16. A. E. Gash, T. M. Tillotson, J. H. Satcher Jr, L. W. Hrubesh, R. L. Simpson, New sol–gel synthetic route to transition and main-group metal oxide aerogels using inorganic salt precursors*, J. Non-Cryst. Solids*., 285(2001), 22-28.
17. U. Balachandran, R. W. Siegel, Y. X. Liao, T. R. Askew, Synthesis, sintering, and magnetic properties of nanophase Cr_2O_3, *Nanostruct. Mater*., 5 (1995), 505-512.
18. Y. Xia, R. Mokaya, Hollow spheres of crystalline porous metal oxides: A generalized synthesis route via nanocasting with mesoporous carbon hollow shells*, J. Mater. Chem*., 15(2005), 3126-3131.
19. D. Vollath, D. V. Szabó, J. O. Willis, Magnetic properties of nanocrystalline Cr_2O_3 synthesized in a microwave plasma, *Mater. Lett*., 29(1996), 271-279.
20. D. Jasaitis, A. Beganskienė, J. Senvaitienė, A. Kareiva, R. Ramanauskas, R. Juškėnas, A. Selskis, Sol-gel synthesis and characterization of cobalt chromium spinel $CoCr_2O_4$, *Chemija*., 22 (2011), 125-130.
21. S. K. Durrani, S. Z. Hussain, K. Saeed, Y. Khan, M. Arif, N. Ahmed, Hydrothermal synthesis and characterization of nanosized transition metal chromite spinels, *Turkish J. Chem*., 36(2012), 111-120.
22. Y. Xiong, X. Lu (Eds), Metallic Nanostructures: From Controlled Synthesis to Applications, *Springer*.,

(2014).
23. C. Ramesh, K. Mohan Kumar, N. Latha, V. Ragunathan, V, Green Synthesis of Cr2O3 Nanoparticles Using Tridax procumbens Leaf Extract and its Antibacterial Activity on Escherichia coli, *Current Nanoscience*, 8(2012), 603-607.
24. C. Feldmann, Polyol-Mediated Synthesis of Nanoscale Functional Materials, *Adv. Funct. Mater.,* 13(2003), 101-107.
25. P. E. Wretblad, Röntgenographische Untersuchung der Systeme Fe_2O_3-Cr_2O_3 und Fe_2O_3-Mn_2O_3, *Z. Anorg. Allg. Chemie*., 189(1930), 329-336.
26. W. Cai, J. Wan, Facile synthesis of superparamagnetic magnetite nanoparticles in liquid polyols*, J. Colloid Interface Sci*., 305(2007), 366–370.
27. A. Malecki, B. Malecka, R. Gajerski and S. £abu, Thermal Decomposition Of Chromium (III) Nitrate (V) Nanohydrate, *J. Therm. Anal. Calorim*., 72 (2003), 135-144.
28. S. Lei, L. Liu, C. Wang, X. Shen, C. Wang, D. Guo, S. Zeng, B. Cheng, Y. Xiaoa, L. Zhoua, A facile in situ reduction route for preparation of spinel $CoCr_2O_4$ polycrystalline nanosheets and their magnetic properties*, Cryst. Eng. Comm.*, 16(2014), 277–286.
29. A. Fallah Shojaei, A. Roshan Tabari, M. H. Loghmani, Normal spinel $CoCr_2O_4$ and $CoCr_2O_4$/TiO_2 nanocomposite as novel photocatalysts for degradation of dyes*, Micro Nano Letters.*, 8(2013), 426–431.
30. T. F. Tadros, Applied Surfactants: Principles and Applications, John Wiley & Sons., (2005), 285-308.

How to cite this article:
A. Babaei Darani, M. Khajeh Aminian, H. Zare, Synthesis and Characterization of Two Green Nanopigments Based on Chromium Oxide. Prog. Color Colorants Coat., 10 (2017), 141-148.